Benzo[a]pyrene-induced nitric oxide production acts as a survival signal targeting mitochondrial membrane potential

Kevin Hardonnière, Laurence Huc, Normand Podechard, Morgane Fernier, Xavier Tekpli, Isabelle Gallais, Odile Sergent, Dominique Lagadic-Gossmann

Benzo[a]pyrene-induced nitric oxide production acts as a survival signal targeting mitochondrial membrane potential

Kévin Hardonnière[1,2], Laurence Huc[3], Normand Podechard[1,2], Morgane Fernier[1,2], Xavier Tekpli[4], Isabelle Gallais[1,2], Odile Sergent[1,2], Dominique Lagadic-Gossmann[1,2]

[1]*UMR Inserm 1085, Institut de Recherche en Santé, Environnement et Travail (IRSET), Rennes, France;*

[2]*Université de Rennes 1, SFR Biosit, Rennes, France;*

[3]*INRA, ToxAlim (Research Centre in Food Toxicology), 180 chemin de Tournefeuille, BP 93173, F-31027 Toulouse, France; Université de Toulouse, INP, UPS, TOXALIM, 31027 Toulouse, France.*

[4]*Stem Cell Group, Nordic EMBL PartnershipCentre for Molecular Medicine Norway (NCMM), University of Oslo, Oslo, Norway.*

Running title: NO as a survival signal upon benzo[a]pyrene exposure

To whom correspondence should be addressed:
Dr. Dominique Lagadic-Gossmann,
Inserm U1085 / IRSET,
Université Rennes 1,
Faculté de Pharmacie,
2 avenue du Professeur Léon Bernard,
35043 Rennes cedex, France;
Tel: +33(0)223234837;
Fax: +33(0)2 23 23 50 55
E-mail: dominique.lagadic@univ-rennes1.fr

Key words: benzo[a]pyrene, nitric oxide, mitochondrial membrane hyperpolarization, AhR, apoptosis, survival

Abbreviations : AhR, aryl hydrocarbon receptor; B[a]P, benzo[a]pyrene; ΔΨm: mitochondrial membrane potential; iNOS: inducible nitric oxide synthase; P450, cytochrome P450 ; PAH, polycyclic aromatic hydrocarbon

ABSTRACT

Benzo[a]pyrene (B[a]P), the prototype molecule of polycyclic aromatic hydrocarbons, exhibits genotoxic and carcinogenic effects, which has led the International Agency for Research on Cancer to recognize it as a human carcinogen. Besides the well-known apoptotic signals triggered by B[a]P, survival signals have also been suggested to occur, both signals likely involved in cancer promotion. Our previous work showed that B[a]P induced an hyperpolarization of mitochondrial membrane potential (ΔΨm) in rat hepatic epithelial F258 cells. Elevated ΔΨm plays a role in tumor development and progression, and nitric oxide (NO) has been suggested to be responsible for increases in ΔΨm. The present study therefore aimed at evaluating the impact of B[a]P on NO level in F258 cells, and at testing the putative role for NO as a survival signal, notably in link with ΔΨm. Our data demonstrated that B[a]P exposure resulted in an NO production which was dependent upon the activation of the inducible NO synthase. This enzyme activation involved AhR and possibly p53 activation. Preventing NO production not only increased B[a]P-induced cell death but also blocked mitochondrial hyperpolarization. This therefore points to a role for NO as a survival signal upon B[a]P exposure, possibly targeting ΔΨm.

INTRODUCTION

Polycyclic aromatic hydrocarbons (PAHs) such as benzo[a]pyrene (B[a]P) are major environmental contaminants, notably found in ambient air, cigarette smoke and smoked food. The prototype molecule of PAHs, B[a]P, is well-known to exhibit diverse genotoxic and carcinogenic effects, which has led the International Agency for Research on Cancer to recognize it as a human carcinogen from group 1 (IARC, 2010). Indeed, notably due to its metabolism by cytochromes P450 into reactive molecules and reactive oxygen species (ROS), B[a]P can trigger the formation of DNA adducts or lead to DNA oxidative alterations (Baird et al., 2005; Wells et al., 1997; Zedeck, 1980). Such a genotoxic action along with non-genotoxic effects of B[a]P may be important for the final outcome: cell survival and possible mutations, or apoptosis (Huc et al., 2006, Salas and Burchiel, 1998, Solhaug et al., 2004). So far, our work has mainly dealt with the early mechanisms underlying the apoptosis induced by low concentrations of B[a]P in hepatic cells (F258 rat hepatic epithelial cells and rat primary hepatocytes) (Huc et al., 2006, 2007; Collin et al., 2014). We have thus demonstrated the involvement of two main pathways leading to apoptosis: a DNA damage-related p53 pathway and a membrane remodelling-dependent Na+/H+ exchanger 1 (NHE1) pathway, both involved in mitochondrial alterations (Huc et al., 2006, 2007; Tekpli et al., 2010a). Besides pro-apoptotic signals, B[a]P *per se* or its reactive metabolites have also been demonstrated to elicit anti-apoptotic/survival signals, such as activation of the AKT pathway, inhibition of the pro-apoptotic protein Bad, increase in intercellular communication, up-regulation of RIP1 (Solhaug et al., 2004; Tekpli et al., 2010b; Wang et al., 2013). All these signals might favor the promotion step of the carcinogenic process.

Diverse studies have shown that an elevation of mitochondrial membrane potential (ΔΨm) is a characteristic of tumor development and progression. For example, an elevated intrinsic ΔΨm in colon carcinoma cells has been involved in the enhanced survival capacity of the cells e.g. in response to hypoxia, thereby avoiding apoptosis, escaping anoikis, and invading the basement membrane (Heerdt, 2006). Regarding B[a]P, our previous results have evidenced such an increase in ΔΨm in F258 rat hepatic epithelial cells exposed to this carcinogen (Huc et al., 2003; Holme et al., 2007). The F258 cell line is of particular interest since, due to its high constitutive expression of CYP1B1, it is sensitive to low B[a]P concentrations, and hence might reveal low dose effects relevant to environmental exposure (Holme et al., 2007). Although the B[a]P-induced mitochondrial hyperpolarization in F258 cells appears to depend on the p53 pathway (Huc et al., 2003), its origin remains to be thoroughly analyzed. We have thus hypothesized that nitric oxide (NO) might be responsible for B[a]P-induced increase in ΔΨm, since NO has already been proposed as a regulator of ΔΨm (Beltrán et al., 2002; Nagy et al., 2003). Indeed, B[a]P is known to induce the inducible NO synthase (iNOS) (Chen et al., 2005a, b), and NO has also been described to be a pro-survival signal during carcinogenesis (Choudhari et al., 2013). In this context, this study has been carried out in order to test whether B[a]P induced an NO production in F258 cells, and if so, whether such a production might play a role as a survival signal, by targeting mitochondria.

Our present data show for the first time that B[a]P induced an AhR/p53-dependent NO production *via* iNOS induction, and that NO may play a role as a survival signal in F258 cells, possibly through regulating ΔΨm.

Experimental procedures

Chemicals

Benzo[a]pyrene (B[a]P), α-naphthoflavone (α-NF), 1-Methyl-N-[2-methyl-4-[2-(2-methylphenyl)diazenyl]phenyl-1H-pyrazole-5-carboxamide (CH223191), DEVD-AMC (Asp-Glu-Asp-7-amino-4-methylcoumarin), 3,3'-Dihexyloxacarbocyanine Iodide ($DiOC_6(3)$),Carbonyl cyanide 4-(trifluoromethoxy) phenylhydrazone (FCCP), NG-Methyl-L-arginine acetate salt (LNMMA), 1,1-Diethyl-2-hydroxy-2-nitroso-hydrazine sodium, 2-(N,N-Diethylamino)-diazenolate 2-oxide sodium salt hydrate (NONOate), pifithrin α (PFT- α), N-Acetyl-3-(nitrosothio)-DL-valine, S-Nitroso-N-acetylpenicillamine (SNAP), 2,3,7,8-Tetrachlorodibenzo-p-dioxin solution (TCDD) were all purchased from Sigma Chemical Co. (St. Louis, MO). N-(Diaminomethylene)-4-isopropyl-3-(methylsulfonyl) benzamide (Cariporide) was purchased from Santa Cruz (Frankfurt, Germany). 4,5-Diaminofluorescein Diacetate (DAF-2DA) was purchased from Calbiochem. Hoechst 33342, 4-Amino-5-Methylamino-2′,7′-Difluorofluorescein Diacetate (DAF-FM) and MitoTracker Red CMXROS were purchased from Life Technologies (Saint-Aubin, France). All these products were used as a stock solution in DMSO; final concentration of this vehicle in culture medium was <0.00005% (v/v), and control cultures received the same concentration of vehicle as treated cultures. Rabbit iNOS antibody (ab3523) was purchased from Abcam (Paris, France), mouse monoclonal p21 antibody ([F-5] : sc-6246) from Santa Cruz, and rabbit polyclonal CYP1B1 antibody (CYP1B11-A) from Alpha Diagnostic Intl (San Antonio, USA). Secondary antibodies conjugated to horseradish peroxidase were purchased from DAKO (Les Ulis, France).

Cell culture

The present study was performed on the F258 rat liver epithelial cell line. This cell line was originally initiated from normal liver of 10-day old Fischer rats (Morel-Chany et al., 1978, 1985). Following several culture passages, some of the cells underwent spontaneous transformation (Morel-Chany et al., 1978, 1985). Despite such a transformation, we found that the F258 cells exhibited a relatively normal karyotype with a predominantly diploid population (Supplementary Figure 1), and was still capable of responding to B[a]P-induced DNA damage as witnessed by the p53 activation leading to cell death (Huc et al., 2006). The choice for these cells was supported by the fact that we previously described it to be sensitive to low concentrations of B[a]P, due to a high constitutive expression of CYP1B1; note that CYP1A1 protein was not detected even upon high concentrations of B[a]P (Holme et al., 2007). The F258 cell line was cultured in Williams' E medium supplemented with 10% fetal calf serum, 2 mM L-glutamine, at 37°C under a 5% CO_2 atmosphere and treated 24 h following seeding, as previously described (Huc et al., 2004; Payen et al., 2001). B[a]P treatments were performed for 24, 48 and 72 h.

Analysis of NO production in F258 cells

-*Measurement of intracellular NO by flow cytometry:* Intracellular NO was measured by flow cytometry using DAF-FM diacetate. After B[a]P treatment, cells were trypsinized, and stained for 40 min at 37 °C with DAF-FM (5 µM) in HEPES-buffered solution for further analysis using a FACSCalibur flow cytometer (BD Bioscience). NONOate was used as a positive control for NO production and detection (2.5 mM, 40 min incubation). Each measurement was conducted on 40,000 events in the FL1 (530/30 nm) channel and

analyzed with Cell Quest software (BD Bioscience). Live cells were gated according to an FSC/SSC dot plot, by excluding low FSC/SSC events.

-*iNOS immunostaining & imaging:* F258 cells, grown on coverslips, were stained with 40 nM Mitotracker Red during the last 30 min of B[a]P exposure. Cells were next washed with PBS and fixed in 4% paraformaldehyde (Sigma–Aldrich) for 20 min and then washed with PBS. Cells were next pre-incubated with PBS containing 4% bovine serum albumin and 0.4% saponin for 1 h, prior to incubation overnight with 10 µg/mL anti-iNOS antibody or with isotype-control. After washing in PBS, cells were incubated for 2 h with secondary Alexa fluor 514 goat anti-rabbit antibody (Life technologies). Samples were digitized with 63x or 40x fluorescence objectives (Zeiss) on the IX83 inverted microscope (Olympus; Rungis, France) equipped with an ultra-high-speed wavelength switching system Lambda DG4 (Sutter Instrument; Novato, USA) and an ORCA Flash 4.0 CMOS camera (Hamamatsu; Massy, France) using cellSense software (Olympus).

-*Determination of NO levels by fluorescence microscopy:* F258 cells grown on glass coverslip were loaded with 40 nM Mitotracker Red and with 10 µM DAF-2/DA during the last 30 min of exposure. After treatment, cells were gently washed twice with HEPES-buffered solution and kept at 37°C before acquisition. As a negative control, cells were incubated in media lacking DAF-2/DA. Processed cells were digitized with 63x or 40x fluorescence objectives (Zeiss) as for iNOS immunostaining (see above).

Cell toxicity estimation

-*Apoptotic cell quantification by fluorescence microscopy:* Number of apoptotic cells was evaluated by fluorescence microscopy through counting cells exhibiting chromatin

condensation and/or fragmentation following staining with the chromatin dye Hoechst 33342. After treatments, cells were stained with 50 µg / ml Hoechst 33342 in the dark for 30 min at 37 °C. Cells were then examined under fluorescence microscopy (Olympus BX60, France). Total population was always more than 400 cells.

-*ATP quantification:* ATP content was evaluated using a luminescence assay kit based upon the reaction of luciferin with ATP in the presence of luciferase (CellTiter-Glo luminescence cell viability assay, Promega; Charbonnieres, France), according to the manufacturer's instructions. The amount of ATP was proportional to the luminescent signal measured with a spectrophotometer (SpectraMax Gemini; Molecular Devices, France).

-*Caspase activity assays:* The caspase-3/7 activity assays were performed using DEVD-AMC tetrapeptide substrate. Caspase activity was measured over a two hours kinetic monitoring of free AMC release at 37°C on a Spectramax Gemini XS plate reader (Molecular Devices). Free AMC detection was performed using 380 nm excitation and 440 nm emission wavelength. Briefly, both adherent and floating F258 cells were lysed in the caspase activity buffer (50 mM HEPES pH 7.5, 150 mM NaCl, 1 mM EGTA pH 7.4, 0.1% Tween, 10% glycerol, 1 mM DTT). Forty µg of crude lysate were then incubated at 37°C in a caspase assay buffer (20 mM PIPES pH 7.2, 100 mM NaCl, 10% sucrose, 1 mM EDTA, 0.1% CHAPS, 1 mM dithiothreitol) containing 80 µM of DEVD-AMC. Three independent experiments, performed in triplicate, were carried out for each experimental condition. Enzyme activities were determined as initial velocities and expressed as relative intensity/hour.

RNA isolation and reverse transcription - real-time quantitative polymerase chain reaction (RT-qPCR) analysis

Total RNA were isolated from F258 cells using the TRIzol method (InVitrogen) and were then subjected to reverse transcription-quantitative polymerase chain reaction (RT-qPCR) analysis, as previously described (Podechard et al., 2008). Gene-specific primers for CYP1B1, GADD45, p21 and 18S were purchased from Sigma, and the sequences used for each gene were as follows: CYP1B1: forward, CAGCTTTTTGCCTGTCACCC - reverse, ATGAAGCCGTCCTTGTCCAG; GADD45: forward, AGATCGAAAGGATGGACACGG – reverse: GGTCGTCATCTTCATCCGCA; p21: forward, CTGGGGAGGGCTTTCTTTGT – reverse, GCCTGTTTCGTGTCTACTGTTC; 18S: forward, CCGGTACAGTGAAACTGCGA – reverse, GATAAATGCACGCGTTCCCC. The amplification curves of the PCR products were analyzed with the ABI Prism SDS software using the comparative cycle threshold method. To assess the successful amplification of each target gene, a standard curve was performed for each primer set. The expression levels of target genes were normalized relative to the expression of an 18S RNA endogenous reference and were given as fold change compared to control with vehicle (DMSO).

Western blotting

After treatment, cells were harvested and lysed for 20 min on ice in RIPA buffer supplemented with 1 mM phenylmethylsulfonyl fluoride, 0.5 mM dithiothreitol, 1 mM orthovanadate, and a cocktail of protein inhibitors (Roche). Cells were then centrifuged at 13,000g for 15 min at 4 °C. Thirty µg of whole-cell lysates were heated for 5 min at 100 °C, loaded in a 4% stacking gel, and then separated by 10% sodium dodecyl sulfate–polymerase gel electrophoresis (SDS–PAGE). Gels were electroblotted overnight onto

nitrocellulose membranes (Millipore). After membrane blocking with a Tris-buffered saline (TBS) solution supplemented with 5% bovine serum albumin, membranes were hybridized with primary antibodies against p21 or CYP1B1 overnight at 4 °C, and next incubated with appropriate horseradish peroxidase-conjugated secondary antibodies for 1 hour. For protein loading evaluation, primary antibodies against HSC70 or β-actin were used. Immunolabeled proteins were then visualized by chemiluminescence using the LAS-3000 analyzer (Fujifilm). Image processing was performed using Multi Gauge software (Fujifilm).

Determination of the Mitochondrial Membrane Potential (Δψm)

Mitochondrial membrane potential $\Delta\Psi_m$ was measured by flow cytometry using $DiOC_6(3)$. After treatment, cells were trypsinized, stained for 20 min at 37 °C with $DiOC_6(3)$ (50 nM) in HEPES-buffered solution, and next analyzed using a FACSCalibur flow cytometer (BD Bioscience). FCCP was used as an uncoupling control (50 μM, 20 min incubation). Each measurement was conducted on 40,000 events in the FL1 (530/30 nm) channel and analyzed with Cell Quest software (BD Bioscience). Live cells were gated according to an FSC/SSC dot plot, by excluding low FSC/SSC events.

Statistical analysis

Data were obtained from a minimum of three independent experiments. All data are quoted as mean ± SD. Analysis of variance followed by Newman–Keuls test was used to test the effects of B[a]P. Differences were considered significant at the level of $P < 0.05$. All statistical analysis were performed using GraphPad Prism 5.01 Software (GraphPad Software, San Diego, USA).

RESULTS

1- An iNOS-dependent NO production is triggered by B[a]P exposure of F258 rat hepatic epithelial cells, and depends on both AhR and p53.

In order to test the effect of B[a]P on endogenous NO, we first used the fluorescent probe DAF-FM and flow cytometry. As shown in Figure 1, B[a]P induced a rightward shift of the fluorescent peak, like the positive control 1,1-Diethyl-2-hydroxy-2-nitroso-hydrazine sodium, 2-(N,N-Diethylamino)-diazenolate 2-oxide sodium salt hydrate (NONOate), from 24h, still detected at 72h, thus indicating an NO production. In order to confirm such a production, another NO-sensitive fluoroprobe, namely DAF2-DA, was also used with detection in fluorescence microscopy. Data in Supplementary Figure 2A confirm such a result, with the appearance of green fluorescence upon B[a]P, similar to what was observed upon NONOate exposure. To firmly validate the B[a]P-induced NO production and due to the fact that some interference can exist between ROS and DAF-FM (Balcerczyk et al., 2005), exogenous application of known antioxidant molecules, namely superoxide dismutase (SOD)-PEG and catalase-PEG were tested; as shown in Supplementary Figure 2B, the rightward shift of the DAF-FM fluorescent peak remained unaffected by both compounds, thus validating the B[a]P-induced NO production. We next decided to test the possible involvement of B[a]P metabolism via CYP1 and/or AhR (known to be activated by B[a]P; Nebert et al., 2000), and p53 in the NO production. It is noteworthy that in F258 cells, AhR appeared to be not significantly involved in the regulation of CYP1B1 protein level as previously described (Tekpli et al., 2010a), and confirmed in the present work (Supplementary Figure 3A). As shown in Figure 1, α-naphthoflavone as well as pifithrin-α fully prevented the B[a]P-induced rightward shift

of the DAF-FM fluorescent peak, related to NO production. With respect to AhR, Supplementary Figure 4A clearly showed that the specific inhibitor of AhR, CH223191, prevented the B[a]P-induced NO production. Furthermore, as illustrated in Supplementary Figure 4B, TCDD, a potent activator of AhR, was also capable of inducing an NO production, thus confirming the involvement of AhR. Finally, as a few studies also suggested a role for Na^+/H^+ exchanger in the regulation of NO production (Ishizaki et al., 2008), and as this exchanger has been shown to be activated by B[a]P in F258 cells (Huc et al., 2004), a possible role for NHE1 was also tested using cariporide. Data in Supplementary Figure 5 clearly showed that inhibition of NHE1 by cariporide was ineffective towards preventing the B[a]P-induced NO production.

The next set of experiments was performed in order to test the possible involvement of the inducible NO synthase (iNOS) in the B[a]P-induced NO production in F258 cells. To do so, the induction of iNOS upon B[a]P was first studied by immunofluorescence using a primary antibody specifically targeting the iNOS and a secondary fluorescent antibody (see Experimental procedures). As shown in Figure 2A, a strong induction of iNOS was observed upon B[a]P exposure as soon as 24h, as visualized by the marked increase of the green fluorescence in the cytoplasm compared to control cells. Such an effect was also observed after a 48h exposure.

Regarding the possible mechanisms involved in iNOS induction, similarly to NO production, this induction observed at 48h was found to be prevented by α-naphthoflavone, CH223191 (CH; Figure 2B) and pifithrin-α (PIF; Figure 2C), but remained unaffected by cariporide (Car; Figure 2C).

Altogether, these results indicated that B[a]P exposure resulted in an NO production in F258 cells that relied upon an AhR/p53-dependent induction of iNOS.

2- The B[a]P-induced NO production represents a survival signal which slows down the development of the related cell death.

As NO is a known regulator of the balance between cell death and survival (Choudhari et al., 2013; Burke et al., 2013), we then decided to test the role of NO in the toxic effects induced by B[a]P in F258 cells. First, the effect of an exogenous application of NO, through the use of the NO-donor SNAP (50 µM), was tested towards B[a]P-induced apoptosis, as evaluated by Hoechst 33342 staining of the chromatin and cell counting (Figure 3A). As expected from our previous results, cell exposure to B[a]P (50 nM, 72h) led to a significant increase of the number of cells with condensed or fragmented chromatin (to ~22 %). The presence of SNAP however significantly decreased by about 50 % the apoptotic cell number induced by B[a]P exposure. Therefore, application of exogenous NO appeared to be protective. This then led us to test if a similar protection was afforded by the B[a]P-elicited endogenous NO production. As iNOS was induced under our experimental conditions, we decided to test L-NMMA (500 µM), a known inhibitor of NOS, as well as carboxy-PTIO (25 µM), an NO scavenger. As shown in Figure 3B, both compounds significantly enhanced the number of apoptotic cells under B[a]P exposure (by ~ 50 %). This was associated with a further decrease in intracellular ATP level compared to B[a]P alone (Figure 3C). Finally, as NO has been described to alter caspase activation (Liu and Stamler, 1999), the impact of L-NNMA and carboxy-PTIO on B[a]P-induced caspase 3/7 activation was tested (Figure 3D). Our data showed that

inhibiting NO production did not significantly affected the B[a]P-elicited caspase activation.

Taken together, these data suggested that the B[a]P-induced NO production acted as a survival pathway, since its inhibition increased apoptosis independently of caspase 3/7 activation.

3- The NO-related protective effect does not go through an effect on AhR or p53 activations.

In order to test the possible impact of NO on the activation of AhR or p53, we analyzed how specific target genes of AhR and p53 were affected by the presence of the NO donor SNAP or the NO scavenger carboxy-PTIO. Regarding AhR, despite no change of CYP1B1 protein level upon B[a]P (50 nM) exposure (Supplementary Figure 3A and Tekpli et al., 2010a), we previously found an induction of its mRNA expression in F258 cells (Dendelé et al., 2014). As expected, similar results were presently obtained, and inhibiting AhR by CH223191 reduced CYP1B1 induction, both at 24 and 48h, therefore indicating a role for AhR in CYP1B1 mRNA induction upon B[a]P 50 nM. However, no marked effect of NO on the B[a]P-related CYP1B1 mRNA induction was observed since carboxy-PTIO and SNAP were ineffective (Figure 4A). In order to confirm these results, the protein levels of CYP1B1 were evaluated by western blotting. As shown in Figure 4B, manipulating the intracellular NO did not affect CYP1B1 protein level. Note that despite an effect of pifithrin-α on CYP1B1 mRNA expression (Figure 4A), no change was detected at the protein level (Figure 4B). It is also worth noting that in F258 cells, this compound did not prevent early intracellular signals related to B[a]P metabolism such as NHE1

activation (Huc et al., 2007); in this context, this discarded a substantial inhibitory effect of pifithrin-α on the CYP1B1 activity in our cell model.

Regarding the p53 activation, the effect of NO on this activation was tested by analyzing the target gene p21. A slight, but significant, induction in the mRNA expression of p21 was thus observed upon B[a]P 50 nM at 24h (Figure 5A), with no change at 48h (Supplementary Figure 7A), and a clear increase in the level of p21 protein was detected at 48h (Figure 5B). Such a difference in the amplitude of effect might stem from the involvement of other p21 regulating mechanisms in F258 cells, such as prevention of the protein degradation (Warfel and El-Deiry, 2013). Nevertheless, it is worth emphasizing that pifithrin-α was capable of preventing the B[a]P-elicited increase in both mRNA and protein levels thus pointing to a role for p53 in the regulation of p21 expression under our experimental conditions. With regard to a potential effect of NO on p53 activation, no marked effect was observed in the presence of CPTIO or SNAP (Figure 5B). Note that no marked change in GADD45 mRNA expression, another p53 gene target, was also observed following exposure to B[a]P 50 nM when CPTIO or SNAP was tested (Supplementary Figure 7B).

Taken together, these results indicate that the B[a]P-induced endogenous NO production would not interfere with AhR and p53 activation.

4- Inhibition of B[a]P-induced NO production prevented the related AhR and p53-dependent mitochondrial membrane hyperpolarization.

As executive caspases did not seem to be the target of NO, we then decided to focus on mitochondrial membrane potential (ΔΨm). First, the time-course effects of a low

concentration of B[a]P (50 nM) was evaluated on the ΔΨm of F258 cells. As expected from our previous studies (Huc et al., 2003; Holme et al., 2007), an increase in ΔΨm was detected following a 48h exposure to B[a]P, as visualized by the rightward shift of the DiOC6 fluorescent peak measured by flow cytometry, in contrast to the leftward shift induced by the uncoupler molecule FCCP (50 μM) used as positive control for mitochondrial depolarization (Figure 6A). We further demonstrated here that such a hyperpolarizing effect already occurred from 24h, and was still observed at 72h. Using α-naphthoflavone (10 μM), we also showed that B[a]P metabolism and/or AhR activation were involved in this effect on ΔΨm, since this inhibitor prevented any shift of the fluorescent peak upon B[a]P (Figure 6A). As AhR has been previously described to induce mitochondrial hyperpolarization (Tappenden et al., 2011) and appeared to be involved in NO production (Supplementary Figure 4A), we next decided to further test the involvement of this receptor under our experimental conditions. As illustrated in Figure 6A, the specific AhR inhibitor, CH223191 (10 μM), markedly inhibited the mitochondrial hyperpolarization, at all exposure times. A role for AhR was also demonstrated using TCDD (10 nM), a very well-known, strong inducer of AhR. Indeed, Supplementary Figure 6 clearly shows that TCDD led to marked mitochondrial hyperpolarization in F258 cells, starting at 24h. As we have previously shown that p53, but not NHE1, was involved in mitochondrial hyperpolarization observed following a 48h exposure to B[a]P (Huc et al., 2003) and in iNOS-dependent NO production (present data), we tested the effects of pifithrin-α (10 μM) and cariporide (10 μM), two known inhibitors of p53 and NHE1, respectively (Figure 6B). Whereas cariporide did not prevent the rightward shift of DiOC6 fluorescent peak, pifithrin-α totally inhibited it, whatever the exposure time. This therefore confirms and extends our previous data

(Huc et al., 2003). Work by Nagy's group has previously described a role for NO in the mitochondrial hyperpolarization that occurred during T cell activation (Nagy et al., 2003). As B[a]P was presently shown to induce an endogenous NO production, we then decided to test the involvement of NO in the related hyperpolarization. To do so, the NO scavenger carboxy-PTIO (25 μM) was tested (Figure 6C). Our results clearly showed that such a manoeuver markedly prevented mitochondrial hyperpolarization, whatever the exposure time. It is also worth noting that the TCDD-induced NO production was correlated with mitochondrial hyperpolarization (Supplementary Figure 4B).

These results therefore pointed to mitochondrial membrane hyperpolarization as a target for the B[a]P-elicited, iNOS-dependent endogenous NO production.

DISCUSSION

Benzo[a]pyrene, a widespread environmental carcinogen notably found in cigarette smoke, exhaust fumes and grilled meat, induces cancer in multiple organs, including liver (Wester et al., 2012), and has recently been classified as a human carcinogen from group 1 by the International Agency for Research on Cancer (IARC, 2010). Although this xenobiotic has been shown to affect the different steps of tumor development (i.e. initiation, promotion, progression), the intracellular signaling pathways involved remain to be precisely determined. Our previous work has evidenced a p53-dependent increase in ΔΨm in B[a]P-treated F258 rat hepatic epithelial cells (Huc et al., 2003). As an increase in ΔΨm has been related to tumor phenotype (Heerdt et al., 2006), and due to the fact that NO is both a regulator of ΔΨm (Beltrán et al., 2002; Nagy et al., 2003) and a pro-survival signal during carcinogenesis (Choudhari et al., 2013), we then hypothesized that NO might constitute a survival signal upon B[a]P exposure via targeting ΔΨm. In the present study, we demonstrate that, in F258 cells, B[a]P exposure induces an endogenous NO production dependent on AhR, and possibly on p53. Furthermore, we show, for the first time to our knowledge, that the B[a]P-elicited, iNOS-dependent NO production may play an important role as a survival signal following PAH exposure, likely by acting on ΔΨm (Figure 7).

An NO production upon B[a]P has already been described both *in vivo* and *in vitro*. Thus, regarding the *in vivo*, it has been shown from blood collected from rats treated for two weeks with B[a]P, that this PAH was responsible for an increase in nitrite content used as a marker of NO production (Kumar et al., 2006). With respect to *in vitro* data, B[a]P was found to lead to a time (3-24h)- and dose-dependent release of NO from microglial cells, with a significant effect detected from 20 nM B[a]P following a

24h-treatment (Dutta et al., 2010). In the present study, a NO production was also induced by a low concentration of B[a]P (50 nM) in hepatic cells; in addition we further showed that such a production was maintained following a longer exposure time, since still detected following 72h. Such a long-term *in vitro* effect might thus corroborate what has been previously described *in vivo* (Kumar et al., 2006). An upregulation of iNOS expression in polymorphonuclear leukocytes, which appeared to be dependent on cytochrome P450 1A1 (CYP1A1) expression, has been put forward to explain the B[a]P-induced NO production (Kumar et al., 2006). Such an involvement of iNOS was also reported in microglial cells, with an increase in enzyme protein level as soon as 3h of exposure with 0.2 µM B[a]P (Dutta et al., 2010). Induction of iNOS, especially at the protein level, was also detected in B[a]P-treated F258 cells.

As AhR and p53 are both involved in B[a]P effects in F258 cells, we then wanted to know if they were involved in NO production and iNOS induction upon B[a]P. We found that both CH223191 (AhR inhibitor) and pifithrin-α (p53 inhibitor) prevented both the iNOS induction and NO production. With respect to AhR, a recent study also indicated a role for this receptor in the iNOS induction detected in lungs infected by influenza virus, likely through a paracrine mechanism; indeed, whereas AhR was activated in endothelial cells, iNOS induction was observed both in epithelial cells and macrophages, therefore suggesting the involvement of an iNOS regulator released by endothelial cells (Wheeler et al., 2013). In our experiments, as only one cell type exists in F258 cell line, such a paracrine mechanism would be unlikely to occur. A possible transcriptional regulation of iNOS by AhR might be put forward, especially as two putative AhRE within the *inos* promoter might exist (Wheeler et al., 2013). Although NO is well described as targeting the tumor suppressor p53 notably by affecting its protein

stability (Muntané and De la Mata, 2010), our present data also suggested a possible role for p53 in the regulation of iNOS; furthermore, no change in the p53 activation upon NO modulation was observed (Figure 5 and Supplementary Figure 7). A p53-dependent iNOS regulation has been previously reported in primary normal human fibroblasts, but in that case, p53 was shown to be a negative regulator, through inhibition of the iNOS promoter (Forrester et al., 1996). Further experiments will then be necessary to explain these contradictory results, especially as an unspecific effect was recently proposed for the inhibition by pifithrin-α of the lipopolysaccharide (LPS)-induced nitric oxide (NO) production in RAW 264.7 macrophage-like cells (Mendjargal et al., 2013).

Several studies have reported the ambivalent role of NO in the regulation of cell functions. Indeed, depending on diverse parameters (intracellular concentration, chemical redox environment, duration of exposure), NO can exert either cytoprotection or cytotoxicity (Burke et al., 2013). Regarding the role for NO in the cell response induced by B[a]P, our data clearly indicate a role for endogenous NO production as a survival signal in hepatic cells. Indeed, preventing NO production by carboxy-PTIO (NO scavenger) or L-NMMA (iNOS inhibitor) was found to exacerbate the B[a]P-induced death in F258 cells. It is also noteworthy that exogenous application of a NO donor resulted in a decrease of B[a]P-induced cell death; this thus corroborates previous results showing a protective effect of gaseous NO towards B[a]P-induced human lung fibroblast cell apoptosis (Chen et al., 2005a). Such a cytoprotective role for endogenous NO in liver cells has been previously demonstrated, for example in the context of the TGFβ-induced apoptosis in mouse hepatocytes; indeed, this apoptosis was inhibited by the iNOS-related endogenous NO produced upon interleukin 1β/interferon γ exposure (Pan et al., 2009). Likewise, endogenous NO was shown to exhibit possible beneficial

effects in liver during TNF-induced shock in mice; indeed, co-treating mice with both TNF and L-NAME (the NOS inhibitor N^G-nitro-L-arginine methyl ester) or using $iNOS^{-/-}$ mice led to a marked sensitization for TNF liver toxicity (Cauwels and Brouckaert, 2007).

Regarding the role of NO as an inhibitor of cell death, various intracellular mechanisms have been evidenced. Thus, Chen and coworkers have previously shown that the repressive effect of NO on B[a]P-induced cell apoptosis in human lung fibroblast involves inhibition of JNK1 activation (Chen et al., 2005a). Based upon the fact that inhibiting the B[a]P-induced JNK activation was previously found to result in an inhibition of the related apoptosis in F258 cells (Huc et al., 2007), a role for JNK in the protective effect of NO presently detected appears unlikely. Numerous works have shown that NO can inhibit apoptosis by affecting the expression/activity of diverse pro- or anti-apoptotic proteins. Notably, it has been reported that NO either increased the content of the anti-apoptotic protein Bcl-2 in rat aortic endothelial cells exposed to cytokines, or reduced the up-regulation of the pro-apoptotic protein Bax upon UVA exposure (Liu and Stamler, 1999). Such a regulation is unlikely to occur under our experimental conditions since no change in Bcl-2 and Bax protein content was observed upon B[a]P compared to untreated cells (unpublished data). An effect of NO on the activity of caspase-3, a well-known effector protease of apoptosis, might have also been a clue since the activity of this enzyme has been shown to be inhibited by NO through an S-nitrosation in endothelial cells; such an inhibition then hampered the TNFα- or serum depletion-induced apoptosis (Haendeler et al., 1997). However such a mechanism has to be ruled out in the present study since no further increase in the B[a]P-induced caspase activity was detected in the presence of CPTIO or L-NMMA. As B[a]P has been previously

shown to elicit both caspase-dependent and -independent pathways in F258 cells (Huc et al., 2006), it therefore seems that the protective effect of NO in B[a]P-treated F258 cells might stem from the regulation of caspase-independent pathways. NO is known to exhibit anti-oxidant properties by itself or to favor the expression of anti-oxidant molecules (Cauwels and Brouckaert, 2007). In this context and as oxidative stress plays an important role in the activation of the caspase-independent apoptotic pathway in F258 cells exposed to B[a]P through lysosome damage (Huc et al., 2006; Gorria et al., 2008), the NO effect presently detected might have involved a protection towards oxidative stress. Nevertheless, data on the effects of CPTIO and L-NMMA on lipid peroxidation were not conclusive, at least at 48h (data not shown). Furthermore, if NO anti-oxidant properties would have occurred, co-treating cells with B[a]P and SOD- or catalase-PEG should have led to an enhancement of NO level (Supplementary Figure 2B). A mere explanation for the effects of endogenous NO towards B[a]P-induced toxicity might also have been through an impact on AhR or p53 activation. As shown in Figures 4 and 5, such a hypothesis was ruled out since no change in the B[a]P-induced p21 or CYP1B1 expression was detected upon CPTIO or SNAP co-exposure. Finally, one might hypothesize that mitochondrial hyperpolarization would play an important role in the cell protection signaling afforded by the NO protection. Regarding that point, the present study clearly showed that the B[a]P-induced mitochondrial membrane hyperpolarization, which was found to rely upon both AhR and p53, but not NHE1, was prevented when using CPTIO. This therefore clearly indicated that $\Delta\Psi m$ was a target of endogenous NO in our cell model. It is worth noting that mitochondrial hyperpolarization has been related to alterations of the oxidative phosphorylation, evidenced by a decrease in cell respiration (Forkink et al., 2014), with concomitant

stimulation of glycolysis in order to maintain ATP production (Sánchez-Cenizo et al., 2010). A similar link between reduced mitochondrial activity and shift towards glycolysis due to NO has been previously reported, for example in ovarian cancer cells (Caneba et al., 2014; Chang et al., 2014). The involvement of such a metabolic reprogramming upon B[a]P is currently under investigation and should allow unraveling the mechanisms underlying the NO brake effect towards B[a]P-induced apoptosis.

In conclusion, our study points to an important role for the endogenous NO production as a survival signal in B[a]P-exposed hepatic cells, likely through mitochondrial hyperpolarization. The evidence of a protective role for NO production towards B[a]P-elicited cell death, along with the known effects of NO on DNA damage and DNA repair (Mikhailenko and Muzalov, 2013; Tang et al., 2013), might contribute to the carcinogenesis induced by B[a]P in liver.

Acknowledgements

We wish to thank Drs Aubin Penna and Kenji Shoji for their scientific advice on fluorescence imaging, and Dr Doris Cassio for karyotyping experiments. KH was a recipient of a fellowship from French Ministry for Education and Research. We wish to thank the Faculté des Sciences pharmaceutiques et biologiques de Rennes (University of Rennes 1) for financial support to KH, and the Ligue Nationale contre le Cancer (committees 22, 35, 49, 85) for financial support to our work.

REFERENCES

Balcerczyk, A., Soszynski, M., Bartosz, G., 2005. On the specificity of 4-amino-5-methylamino-2',7'-difluorofluorescein as a probe for nitric oxide. Free Radic. Biol. Med. 39, 327-335.

Baird, W.M., Hooven, L.A., Mahadevan, B., 2005. Carcinogenic polycyclic aromatic hydrocarbon-DNA adducts and mechanism of action. Environ. Mol. Mutagen. 45, 106-114.

Beltrán, B., Quintero, M., García-Zaragozá, E., O'Connor, E., Esplugues, J.V., Moncada, S., 2002. Inhibition of mitochondrial respiration by endogenous nitric oxide: a critical step in Fas signaling. Proc. Natl. Acad. Sci. U S A. 99, 8892-8897.

Burke, A.J., Sullivan, F.J., Giles, F.J., Glynn, S.A., 2013. The yin and yang of nitric oxide in cancer progression. Carcinogenesis. 34, 503-512.

Caneba, C.A., Yang, L., Baddour, J., Curtis, R., Win, J., Hartig, S., Marini, J., Nagrath, D., 2014. Nitric oxide is a positive regulator of the Warburg effect in ovarian cancer cells. Cell. Death Dis. 5:e1302.

Cauwels, A., Brouckaert, P., 2007. Survival of TNF toxicity: dependence on caspases and NO. Arch. Biochem. Biophys. 462, 132-139.

Chang, C.F., Diers, A.R., Hogg, N., 2014. Cancer Cell Metabolism and the Modulating Effects of Nitric Oxide. Free Radic. Biol. Med. doi: 10.1016/j.freeradbiomed.2014.11.012. [Epub ahead of print]

Chen, J.H., Chou, F.P., Lin, H.H., Wang, C.J., 2005a. Gaseous nitrogen oxide repressed benzo[a]pyrene-induced human lung fibroblast cell apoptosis via inhibiting JNK1 signals. Arch. Toxicol. 79, 694-704.

Chen, J., Yan, Y., Li, J., Ma, Q., Stoner, G.D., Ye, J., Huang, C., 2005b. Differential requirement of signal pathways for benzo[a]pyrene (B[a]P)-induced nitric oxide synthase (iNOS) in rat esophageal epithelial cells. Carcinogenesis. 26, 1035-1043.

Choudhari, S.K., Chaudhary, M., Bagde, S., Gadbail, A.R., Joshi, V., 2013. Nitric oxide and cancer: a review. World J. Surg. Oncol. 11:118.

Collin, A., Hardonnière, K., Chevanne, M., Vuillemin, J., Podechard, N., Burel, A., Dimanche-Boitrel, M.T., Lagadic-Gossmann, D., Sergent, O., 2014. Cooperative interaction of benzo[a]pyrene and ethanol on plasma membrane remodeling is responsible for enhanced oxidative stress and cell death in primary rat hepatocytes. Free Radic. Biol. Med. 72, 11-22.

Dendelé, B., Tekpli, X., Hardonnière, K., Holme, J.A., Debure, L., Catheline, D., Arlt, V.M., Nagy, E., Phillips, D.H., Ovrebø, S., Mollerup, S., Poët, M., Chevanne, M., Rioux, V., Dimanche-Boitrel, M.T., Sergent, O., Lagadic-Gossmann, D., 2014. Protective action of n-3 fatty acids on benzo[a]pyrene-induced apoptosis through the plasma membrane remodeling-dependent NHE1 pathway. Chem. Biol. Interact. 207, 41-51.

Dutta, K., Ghosh, D., Nazmi, A., Kumawat, K.L., Basu, A., 2010. A common carcinogen benzo[a]pyrene causes neuronal death in mouse via microglial activation. PLoS One. 5, e9984.

Forkink, M., Manjeri, G.R., Liemburg-Apers, D.C., Nibbeling, E., Blanchard, M., Wojtala, A., Smeitink, J.A., Wieckowski, M.R., Willems, P.H., Koopman, W.J., 2014. Mitochondrial hyperpolarization during chronic complex I inhibition is sustained by low activity of complex II, III, IV and V. Biochim. Biophys. Acta. 1837, 1247-1256.

Forrester, K., Ambs, S., Lupold, S.E., Kapust, R.B., Spillare, E.A., Weinberg, W.C., Felley-Bosco, E., Wang, X.W., Geller, D.A., Tzeng, E., Billiar, T.R., Harris, C.C., 1996. Nitric oxide-induced p53 accumulation and regulation of inducible nitric oxide synthase expression by wild-type p53. Proc. Natl. Acad. Sci. U S A. 93, 2442-2447.

Gorria, M., Tekpli, X., Rissel, M., Sergent, O., Huc, L., Landvik, N., Fardel, O., Dimanche-Boitrel, M.T., Holme, J.A., Lagadic-Gossmann, D., 2008. A new lactoferrin- and iron-dependent lysosomal death pathway is induced by benzo[a]pyrene in hepatic epithelial cells. Toxicol. Appl. Pharmacol. 228, 212-224.

Haendeler, J., Weiland, U., Zeiher, A.M., Dimmeler, S., 1997. Effects of redox-related congeners of NO on apoptosis and caspase-3 activity. Nitric Oxide. 1, 282-293.

Heerdt, B.G., Houston, M.A., Augenlicht, L.H., 2006. Growth properties of colonic tumor cells are a function of the intrinsic mitochondrial membrane potential. Cancer Res. 66, 1591-1596.

Holme, J.A., Gorria, M., Arlt, V.M., Ovrebø, S., Solhaug, A., Tekpli, X., Landvik, N.E., Huc, L., Fardel, O., Lagadic-Gossmann, D., 2007. Different mechanisms involved in apoptosis following exposure to benzo[a]pyrene in F258 and Hepa1c1c7 cells. Chem. Biol. Interact. 167, 41-55.

Huc, L., Gilot, D., Gardyn, C., Rissel, M., Dimanche-Boitrel, M.T., Guillouzo, A., Fardel, O., Lagadic-Gossmann, D., 2003. Apoptotic mitochondrial dysfunction induced by benzo(a)pyrene in liver epithelial cells: role of p53 and pHi changes. Ann. N. Y. Acad. Sci. 1010, 167-170.

Huc, L., Rissel, M., Solhaug, A., Tekpli X., Gorria, M., Torriglia, A., Holme, J.A., Dimanche-Boitrel, M.T., Lagadic-Gossmann D., 2006. Multiple apoptotic pathways induced by p53-dependent acidification in benzo[a]pyrene-exposed hepatic F258 cells. J. Cell. Physiol. 208, 527-537

Huc, L., Sparfel, L., Rissel, M., Dimanche-Boitrel, M.T., Guillouzo, A., Fardel, O., Lagadic-Gossmann, D., 2004. Identification of Na+/H+ exchange as a new target for toxic polycyclic aromatic hydrocarbons. FASEB J. 18, 344-346.

Huc, L., Tekpli, X., Holme, J.A., Rissel, M., Solhaug, A., Gardyn, C., Le Moigne, G., Gorria, M., Dimanche-Boitrel, M.T., Lagadic-Gossmann, D., 2007. c-Jun NH2-terminal kinase-related Na+/H+ exchanger isoform 1 activation controls hexokinase II expression in benzo(a)pyrene-induced apoptosis. Cancer Res. 67, 1696-1705.

IARC., 2010. Some non-heterocyclic polycyclic aromatic hydrocarbons and some related exposures. Monogr. Eval. Carcinog. Risks Hum., 92, 1–853.

Ishizaki, M., Kaibori, M., Uchida, Y., Hijikawa, T., Tanaka, H., Ozaki, T., Tokuhara, K., Matsui, K., Kwon, A.H., Kamiyama, Y., Nishizawa, M., Okumura, T., 2008. Protective effect of FR183998, a

Na+/H+ exchanger inhibitor, and its inhibition of iNOS induction in hepatic ischemia-reperfusion injury in rats Shock. 30, 311-317.

Kumar, A., Patel, S., Gupta, Y.K., Singh, M.P., 2006. Involvement of endogenous nitric oxide in myeloperoxidase mediated benzo(a)pyrene induced polymorphonuclear leukocytes injury. Mol. Cell. Biochem. 286, 43-51.

Liu, L., Stamler, J.S., 1999. NO: an inhibitor of cell death. Cell Death Differ. 6, 937-942.

Mendjargal, A., Odkhuu, E., Koide, N., Nagata, H., Kurokawa, T., Nonami, T., Yokochi, T., 2013. Pifithrin-α, a pharmacological inhibitor of p53, downregulates lipopolysaccharide-induced nitric oxide production via impairment of the MyD88-independent pathway. Int. Immunopharmacol. 15, 671-678.

Mikhailenko, V.M., Muzalov, I.I., 2013. Exogenous nitric oxide potentiate DNA damage and alter DNA repair in cells exposed to ionising radiation. Exp. Oncol. 35, 318-324.

Morel-Chany, E., Guillouzo, C., Trincal, G., Szajnert, M.F., 1978. "Spontaneous" neoplastic transformation in vitro of epithelial cell strains of rat liver: cytology, growth and enzymatic activities. Eur. J. Cancer. 14, 1341-1352.

Morel-Chany, E., Lafarge-Frayssinet, C., Trincal, G., 1985. Progression of spontaneous malignant transformation of epithelial rat liver cell lines. Cell. Biol. Toxicol. 1, 11-22.

Muntané, J., De la Mata, M., 2010. Nitric oxide and cancer. World J. Hepatol. 2, 337-344.

Nagy, G., Koncz, A., Perl, A., 2003. T cell activation-induced mitochondrial hyperpolarization is mediated by Ca2+- and redox-dependent production of nitric oxide. J. Immunol. 171, 5188-5197.

Nebert, D.W., Roe, A.L., Dieter, M.Z., Solis, W.A., Yang, Y., Dalton, T.P., 2000. Role of the aromatic hydrocarbon receptor and [Ah] gene battery in the oxidative stress response, cell cycle control, and apoptosis. Biochem. Pharmacol. 59, 65-85.

Pan, X., Wang, X., Lei, W., Min, L., Yang, Y., Wang, X., Song, J., 2009. Nitric oxide suppresses transforming growth factor-beta1-induced epithelial-to-mesenchymal transition and apoptosis in mouse hepatocytes. Hepatology. 50, 1577-1587.

Payen, L., Courtois, A., Langouët, S., Guillouzo, A., Fardel, O., 2001. Unaltered expression of multidrug resistance transporters in polycyclic aromatic hydrocarbon-resistant rat liver cells. Toxicology. 156, 109-117.

Podechard, N., Lecureur, V., Le Ferrec, E., Guenon, I., Sparfel, L., Gilot, D., Gordon, J.R., Lagente, V., Fardel, O., 2008. Interleukin-8 induction by the environmental contaminant benzo(a)pyrene is aryl hydrocarbon receptor-dependent and leads to lung inflammation. Toxicol. Lett. 177, 130-137.

Salas, V.M., Burchiel, S.W., 1998. Apoptosis in Daudi human B cells in response to benzo[a]pyrene and benzo[a]pyrene-7,8-dihydrodiol. Toxicol. Appl. Pharmacol. 151, 367-376.

Sánchez-Cenizo, L., Formentini, L., Aldea, M., Ortega, A.D., García-Huerta, P., Sánchez-Aragó, M., Cuezva, J.M., 2010. Up-regulation of the ATPase inhibitory factor 1 (IF1) of the mitochondrial H+-ATP synthase in human tumors mediates the metabolic shift of cancer cells to a Warburg phenotype. J. Biol. Chem. 285, 25308-25313.

Solhaug, A., Refsnes, M., Låg, M., Schwarze, P.E., Husøy, T., Holme, J.A., 2004. Polycyclic aromatic hydrocarbons induce both apoptotic and anti-apoptotic signals in Hepa1c1c7 cells. Carcinogenesis. 25, 809-819.

Tang, C.H., Wei, W., Hanes, M.A., Liu, L., 2013. Hepatocarcinogenesis driven by GSNOR deficiency is prevented by iNOS inhibition. Cancer Res. 73, 2897-2904.

Tappenden, D.M., Lynn, S.G., Crawford, R.B., Lee, K., Vengellur, A., Kaminski, N.E., Thomas, R.S., LaPres, J.J., 2011. The aryl hydrocarbon receptor interacts with ATP5α1, a subunit of the ATP synthase complex, and modulates mitochondrial function. Toxicol. Appl. Pharmacol. 254, 299-310.

Tekpli, X., Rissel, M., Huc, L., Catheline, D., Sergent, O., Rioux, V., Legrand, P., Holme, J.A., Dimanche-Boitrel, M.T., Lagadic.-Gossmann., D., 2010a. Membrane remodeling, an early event in benzo[a]pyrene-induced apoptosis. Toxicol. Appl. Pharmacol. 243, 68-76.

Tekpli, X., Rivedal, E., Gorria, M., Landvik, N.E., Rissel, M., Dimanche-Boitrel, M.T., Baffet, G., Holme, J.A., Lagadic-Gossmann, D., 2010b. The B[a]P-increased intercellular communication via translocation of connexin-43 into gap junctions reduces apoptosis. Toxicol. Appl. Pharmacol. 242, 231-240.

Wang, Q., Chen, W., Xu, X., Li, B., He, W., Padilla, M.T., Jang, J.H., Nyunoya, T., Amin, S., Wang, X., Lin, Y., 2013. RIP1 potentiates BPDE-induced transformation in human bronchial epithelial cells through catalase-mediated suppression of excessive reactive oxygen species. Carcinogenesis. 34, 2119-2128.

Warfel, N.A., El-Deiry, W.S., 2013. p21WAF1 and tumourigenesis: 20 years after. Curr. Opin. Oncol. 25, 52-58.

Wells, P.G., Kim, P.M., Laposa, R.R., Nicol, C.J., Parman, T., Winn, L.M., 1997. Oxidative damage in chemical teratogenesis. Mutat. Res. 396, 65-78.

Wester, P.W., Muller, J.J, Slob, W., Mohn, G.R., Dortant, P.M., Kroese, E.D., 2012. Carcinogenic activity of benzo[a]pyrene in a 2 year oral study in Wistar rats. Food Chem. Toxicol. 50, 927-935.

Wheeler, J.L., Martin, K.C., Lawrence, B.P., 2013. Novel cellular targets of AhR underlie alterations in neutrophilic inflammation and inducible nitric oxide synthase expression during influenza virus infection. J. Immunol. 190, 659-668.

Zedeck, M.S., 1980. Polycyclic aromatic hydrocarbons: a review. J. Environ. Pathol. Toxicol. 3, 537-567.

FIGURE LEGENDS

Figure 1. Effects of B[a]P exposure on endogenous nitric oxide (NO) production involves both CYP1-metabolism and/or AhR and p53 activation. In the absence of inhibitors, F258 cells were treated or not with B[a]P 50 nM during 24, 48 or 72 h (control). When testing inhibitors, F258 cells were pre-treated for 1 h with α-naphthoflavone (αNF; 10 µM), an inhibitor of both B[a]P-metabolism *via* CYP1 and AhR, or pifithrin α (10 µM), an inhibitor of p53, prior to co-exposure to B[a]P (24, 48 and 72h). Flow cytometry analysis was then performed following cell staining with the fluoroprobe DAF-FM (as described in Experimental procedures). NONOate (10 µM; open blue peak) was used as a positive control for NO production. Histograms of NO production are representative of at least 3 independent experiments.

Figure 2. Effects of B[a]P exposure on iNOS levels and involvement of AhR and p53 activations in these effects. F258 cells were treated or not with B[a]P 50 nM during 24 or 48h. When testing inhibitors, cells were pre-treated with the inhibitor for 1 h and then co-exposed with B[a]P. (A) Effects of B[a]P on iNOS induction at 24 and 48h. (B) Effects of AhR inhibition on B[a]P-induced iNOS level using two different inhibitors: α-naphthoflavone (αNF; 10 µM), an inhibitor of both B[a]P-metabolism *via* CYP1 and AhR, and CH223191 (CH, 10 µM), a specific inhibitor of AhR. (C) Effects of the inhibition of p53 and NHE1 on B[a]P-related iNOS induction using pifithrin α (PIF, 10 µM), an inhibitor of p53, and cariporide (Car; 10 µM), a specific inhibitor of NHE1, respectively. After fixation and permeabilization, immunostaining of cells was performed by incubation of a rabbit monoclonal anti-iNOS antibody followed by an Alexa fluor 514 goat anti-rabbit antibody (as described in Experimental procedures). Cells were then

viewed by fluorescence microscopy (magnification x 120). The experiments were repeated 3 times with similar results. Scale bar, 10 µM.

Figure 3. B[a]P-induced NO production counteracts the related cell toxicity. F258 cells were treated or not with B[a]P 50 nM during 72h. When testing the role of NO, cells were pre-treated for 1 h with (A) the NO-donor SNAP (50 µM), or with (B-D) the NO scavenger carboxy-PTIO (CPTIO, 25 µM) or the NOS inhibitor L-NMMA (500 µM), prior to co-exposure to B[a]P. Following treatments, cell toxicity was evaluated by counting cells with fragmented or condensed chromatin following Hoechst 33342 staining (A-B). In (C), intracellular ATP concentration was evaluated as described in Experimental procedures. (D) Caspase activities (as detected by cleavage of DEVD-AMC) were measured by spectrofluorimetry. Number of experiments ≥ 3 for all conditions. *: $p<0.05$, B[a]P + NO modulator *versus* B[a]P-treated cells; ***: $p<0.001$, B[a]P + NO modulator *versus* B[a]P-treated cells.

Figure 4. Absence of NO effects on the mRNA expression and protein level of CYP1B1 in B[a]P-exposed F258 cells. In the absence of inhibitors or NO modulators, F258 cells were treated or not with B[a]P 50 nM (BP50) or 1 µM (BP1000) during 24h (A) or 48h (A, B). When testing inhibitors or NO modulators, cells were pre-treated for 1 h with CH223191 (CH, 10 µM), a specific inhibitor of AhR, or pifithrin α (PIF, 10 µM), an inhibitor of p53, or the NO scavenger carboxy-PTIO (CPTIO, 25 µM), or the NO-donor SNAP (50 µM), prior to co-exposure to B[a]P 50 nM (BP50) for 24h (A) or 48h (A, B). After treatments, RT-qPCR analysis of CYP1B1 mRNA expression (A) or western-blotting analysis of CYP1B1 protein level (B) were performed (as described in Experimental procedures). mRNA expression was given relative to control cells with vehicle. Number

of experiments ≥ 3 for all conditions. *: p<0.05 and ***: p<0.001: test treatment *versus* untreated control cells.

Figure 5. Absence of NO effects on the mRNA expression and protein level of p21 in B[a]P-exposed F258 cells. In the absence of inhibitors or NO modulators, F258 cells were treated or not with B[a]P 50 nM (BP50) or 1 µM (BP1000) during 24h (A) or 48h (B). When testing inhibitors or NO modulators on the p21 mRNA expression (A), cells were pre-treated for 1 h with CH223191 (CH, 10 µM), a specific inhibitor of AhR, or pifithrin α (PIF, 10 µM), an inhibitor of p53, or the NO scavenger carboxy-PTIO (CPTIO, 25 µM), or the NO-donor SNAP (50 µM), prior to co-exposure to B[a]P 50 nM (BP50) for 48h. When looking at the p21 protein level (B), similar exposures were carried out. After treatments, RT-qPCR analysis of CYP1B1 mRNA expression (A) or western-blotting analysis of CYP1B1 protein level (B) were performed (as described in Experimental procedures). mRNA expression was given relative to control cells with vehicle. Number of experiments ≥ 3 for all conditions, except for B[a]P 1 µM (n=2). *: p<0.05: test treatment *versus* untreated control cells.

Figure 6. B[a]P-induced mitochondrial hyperpolarization (ΔΨm) relies upon the activation of both AhR and p53, and on the endogenous NO production. In the absence of inhibitors, F258 cells were treated or not with B[a]P 50 nM during 24, 48 or 72 h (control) (A-C). When testing inhibitors or NO modulator, (A) cells were pre-treated for 1 h with α-naphthoflavone (αNF; 10 µM), an inhibitor of both B[a]P-metabolism via CYP1 and AhR, or CH223191 (10 µM), a specific inhibitor of AhR, or (B) for 1 h with cariporide (10 µM), a specific inhibitor of NHE1, or pifithrin α (10 µM), an inhibitor of p53, or (C) for 1h with the NO scavenger carboxy-PTIO (CPTIO, 25 µM), prior to co-exposure to B[a]P 50 nM (24, 48 and 72h). After treatments, flow cytometry

analysis was performed following cell staining with the fluoroprobe $DiOC_6(3)$ (as described in Experimental procedures). FCCP (50 μM; open blue peak) was used as a positive control for mitochondrial membrane depolarization (A, C). Histograms of ΔΨm are representative of at least 3 independent experiments for all conditions.

Figure 7. A proposed model for the B[a]P-induced endogenous production and its implication as a survival signal in F258 rat hepatic epithelial cells. B[a]P metabolism *via* the constitutively expressed CYP1B1 leads to the activation of NHE1 transporter and p53 pathway, both triggering apoptotic cell death. Note that AhR activation by B[a]P, along with the reactive oxygen species (ROS) production related to CYP metabolism, has been shown to be involved in NHE1 activation, by acting on membrane remodeling (Tekpli et al., 2010a). In parallel, both AhR and p53 activations induce iNOS expression, thereby resulting in an endogenous NO production. Such a production hampers the cell death development, likely by hyperpolarizing mitochondrial membrane.

Figure 1

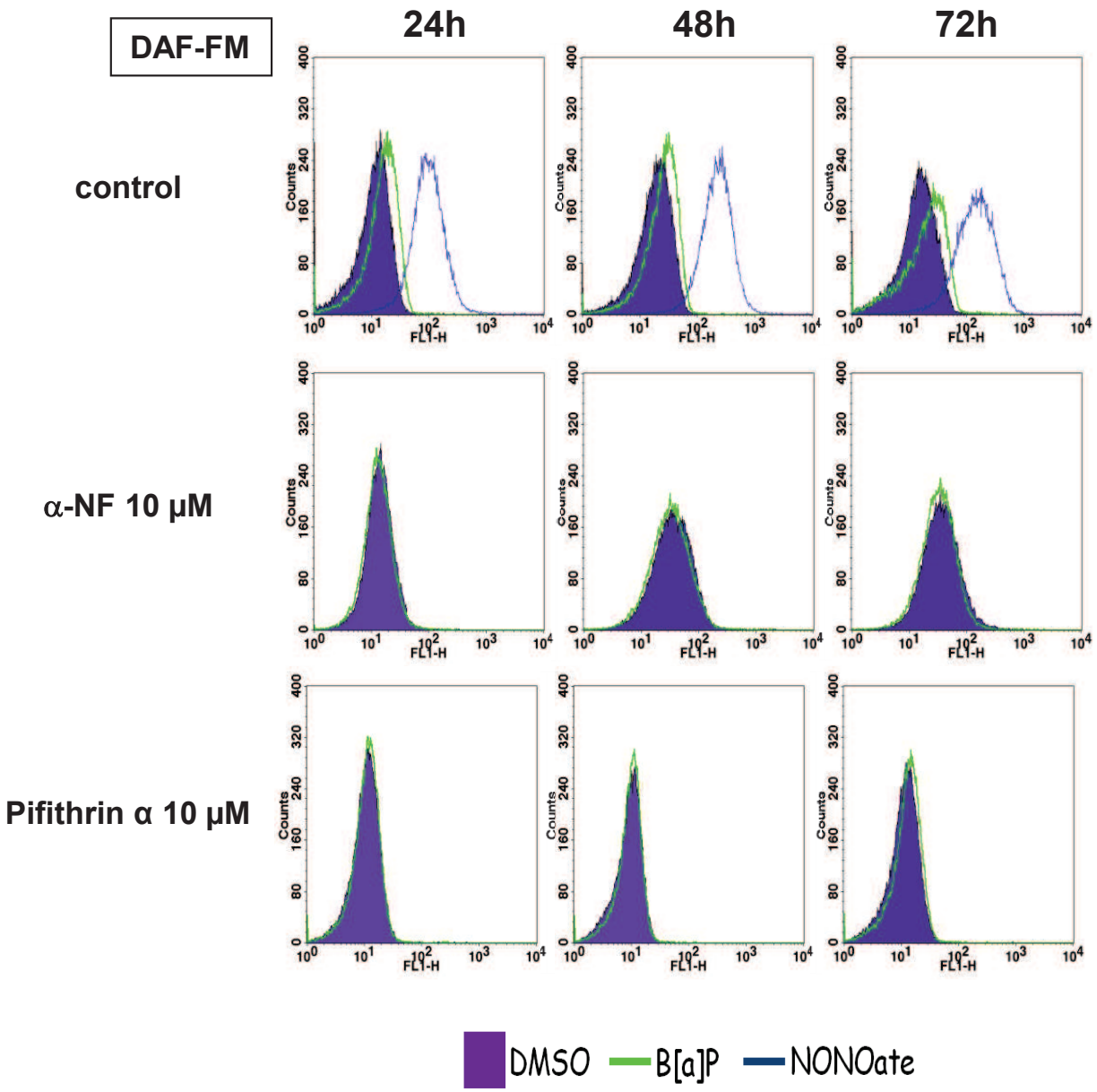

Figure 1

Figure 2

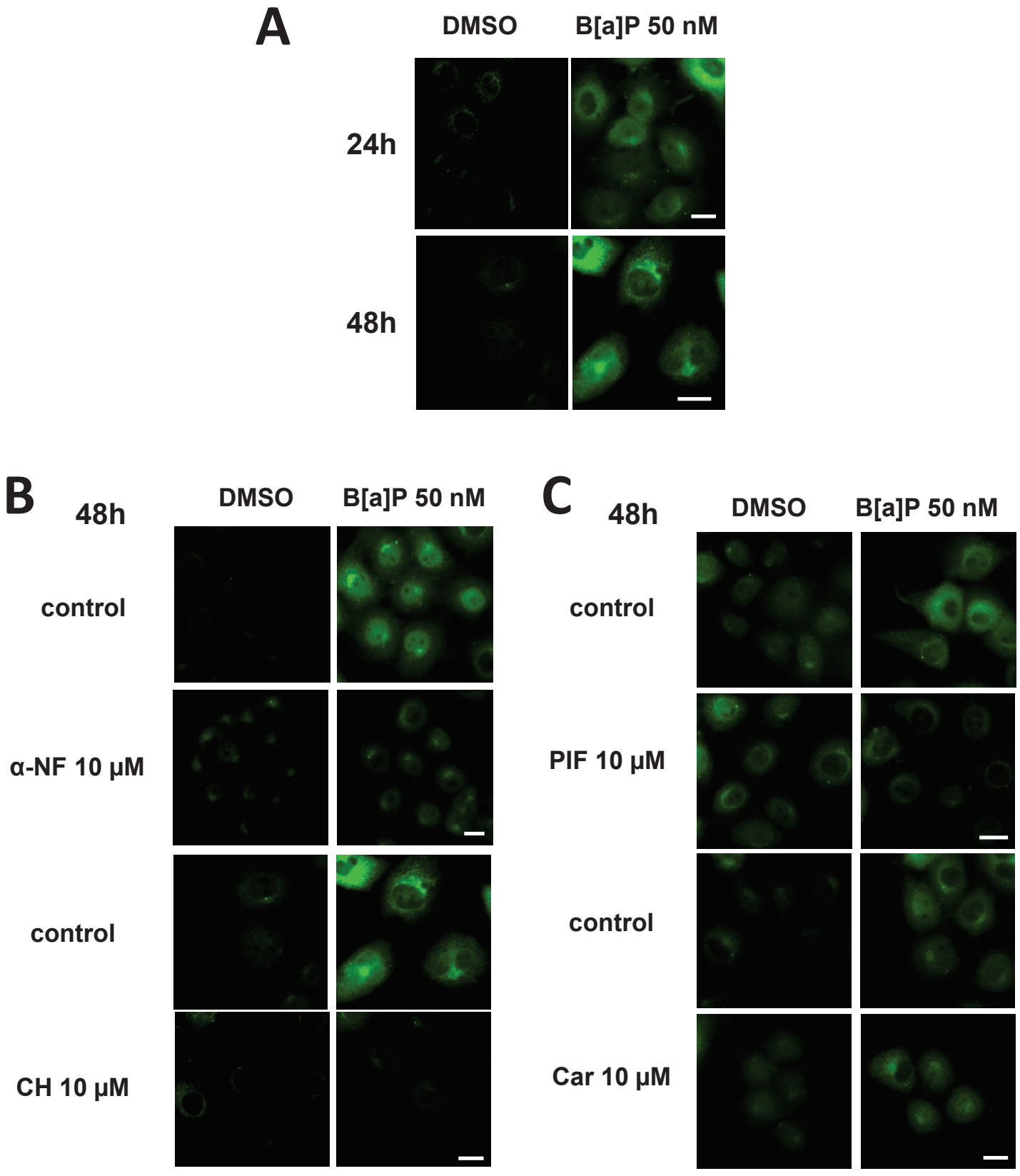

Figure 2

Figure 3

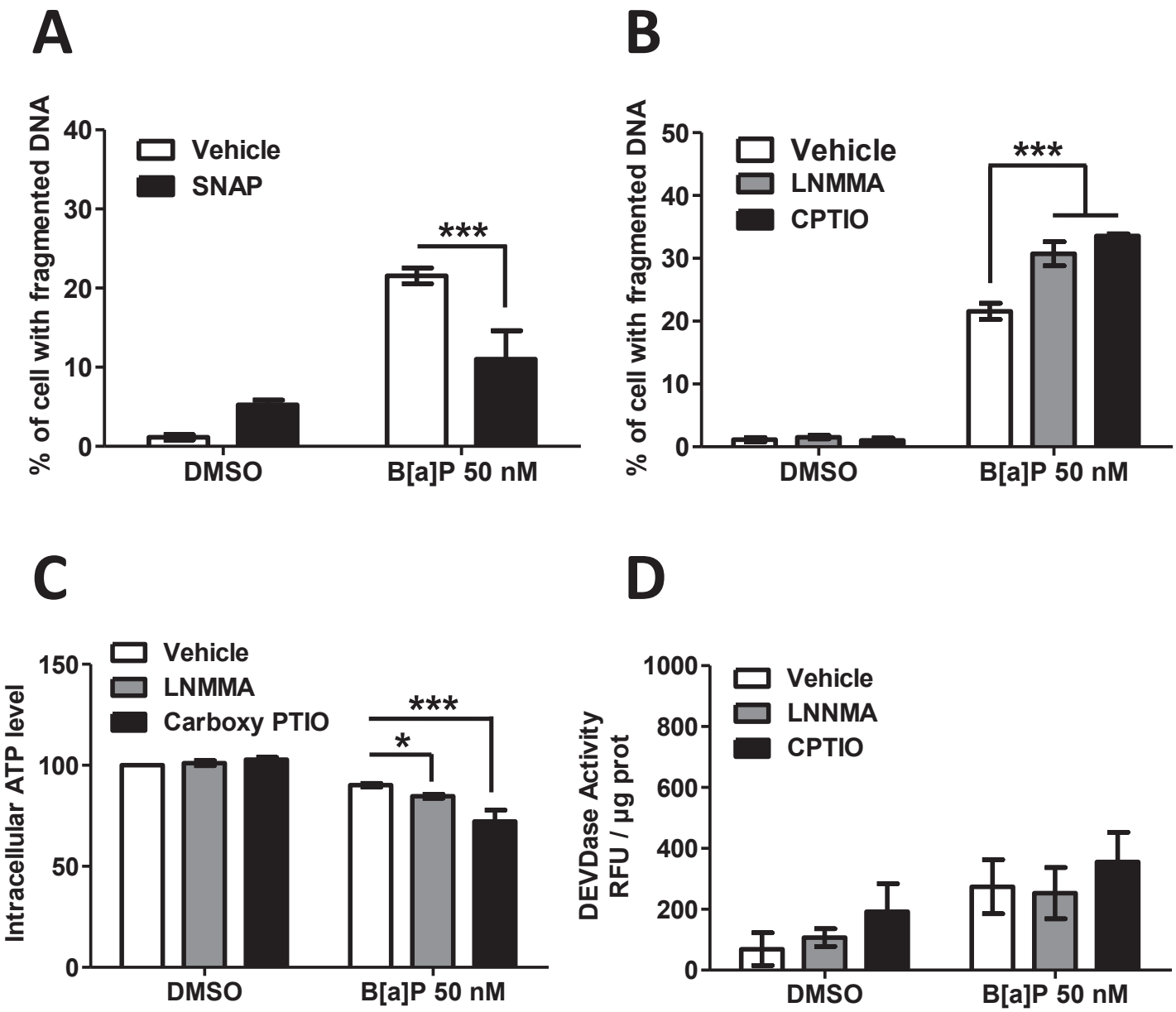

Figure 3

Figure 4

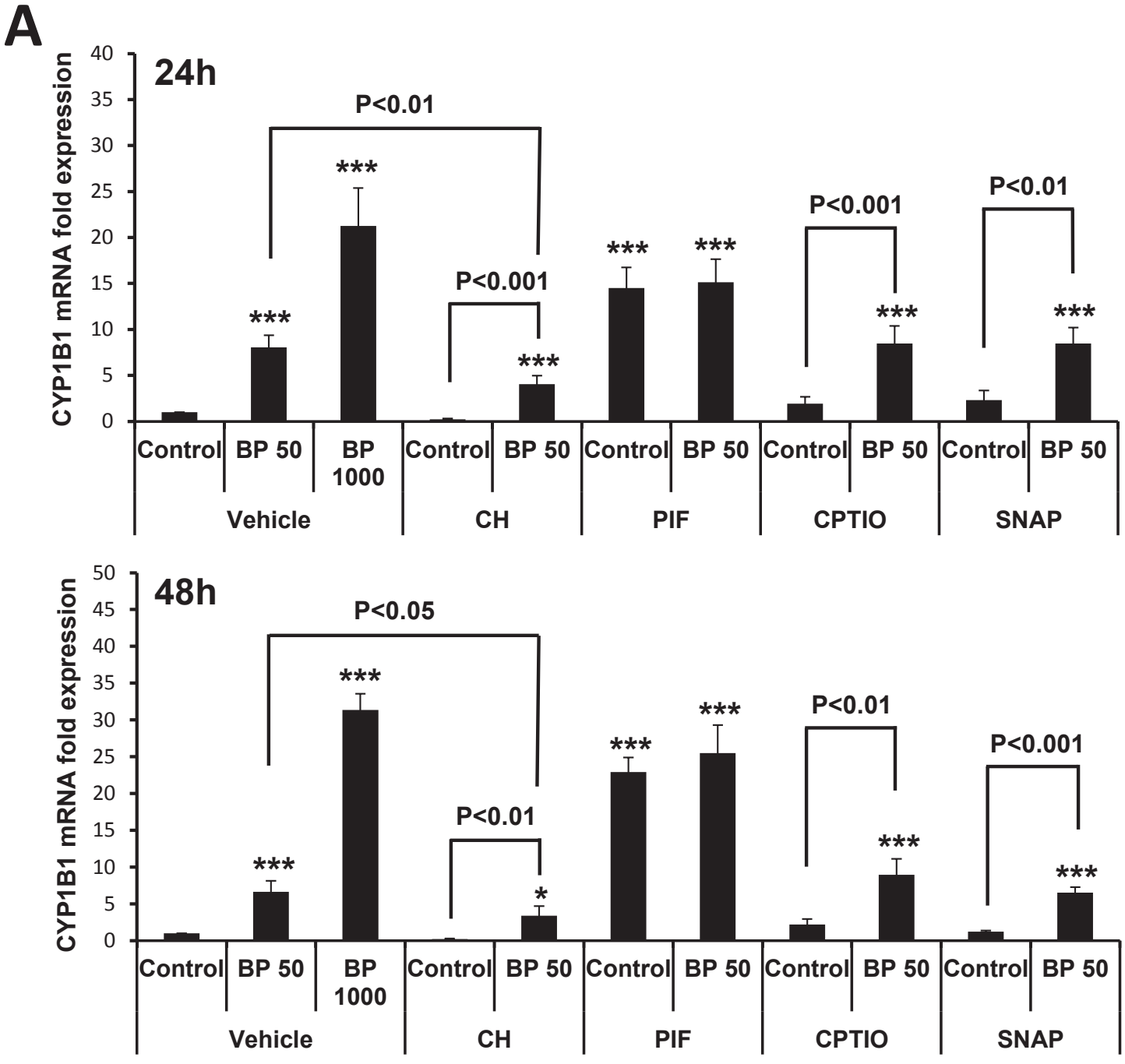

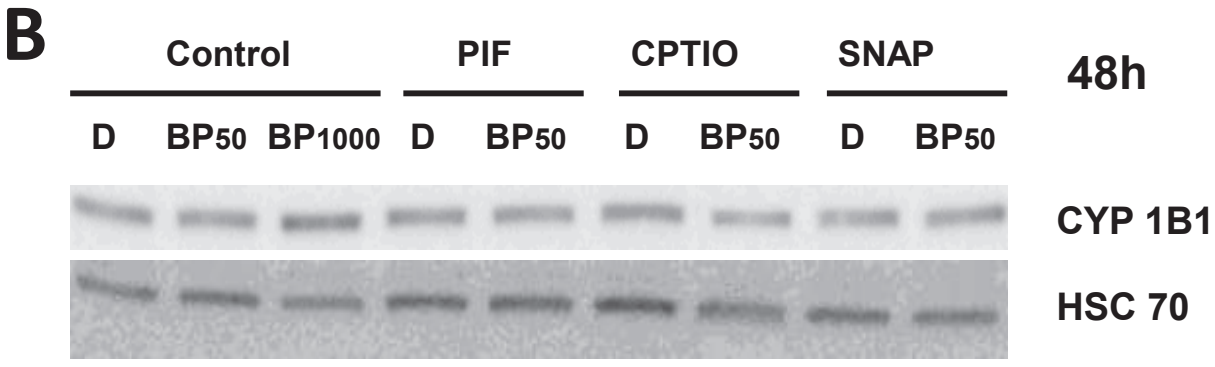

Figure 4

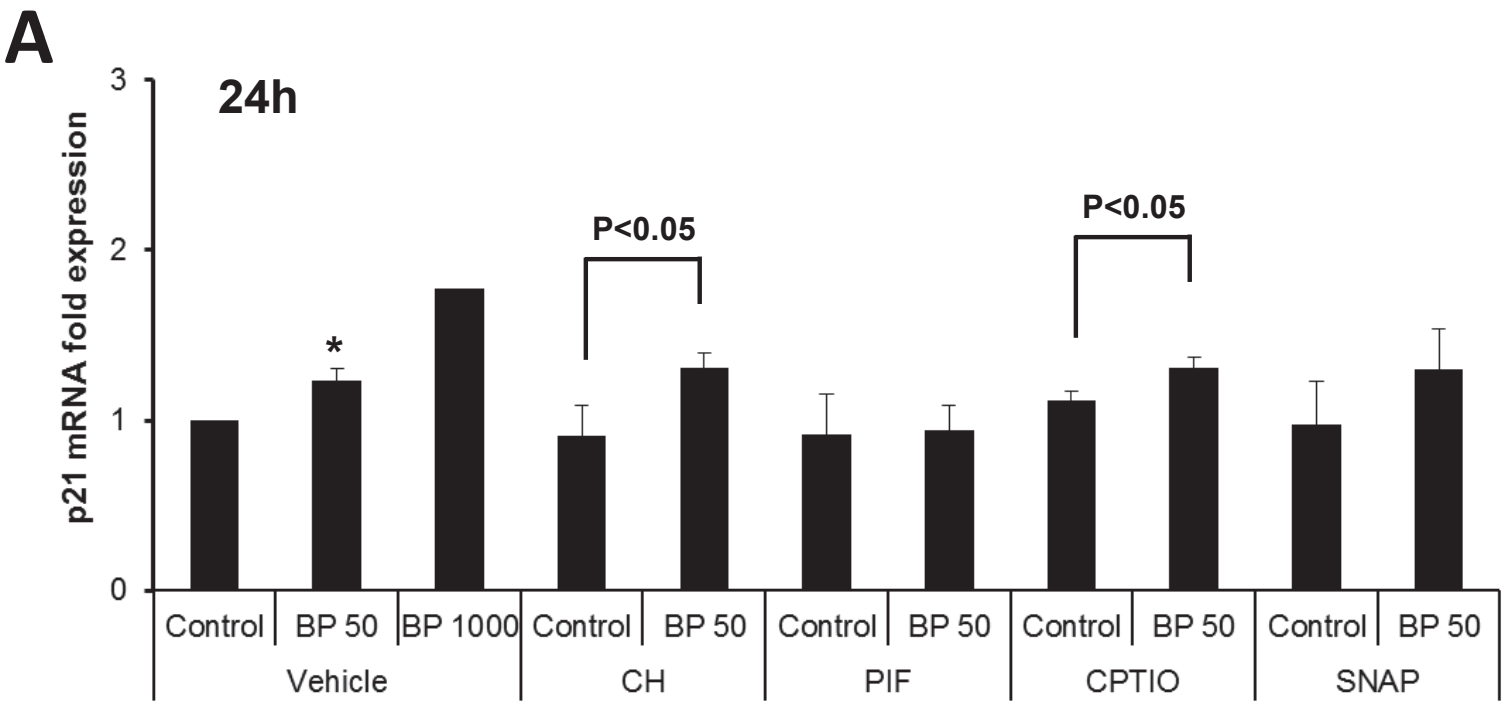
A
24h
p21 mRNA fold expression
3
2
1
0
*
P<0.05
P<0.05
Control
BP 50
BP 1000
Control
BP 50
Control
BP 50
Control
BP 50
Control
BP 50
Vehicle
CH
PIF
CPTIO
SNAP

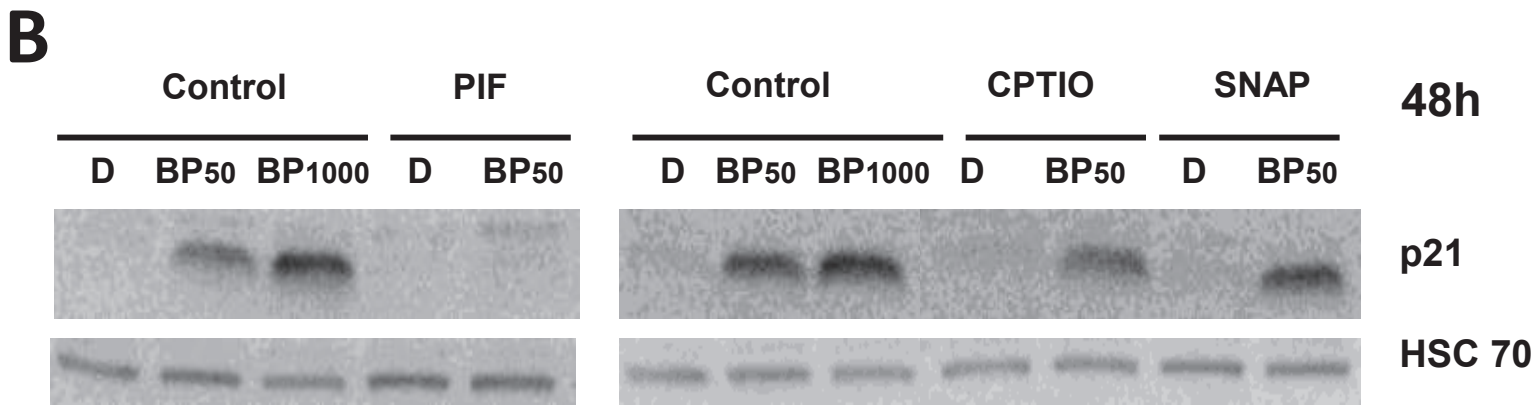
B
Control
PIF
Control
CPTIO
SNAP
48h
D
BP50
BP1000
D
BP50
D
BP50
BP1000
D
BP50
D
BP50
p21
HSC 70

Figure 5

Figure 6

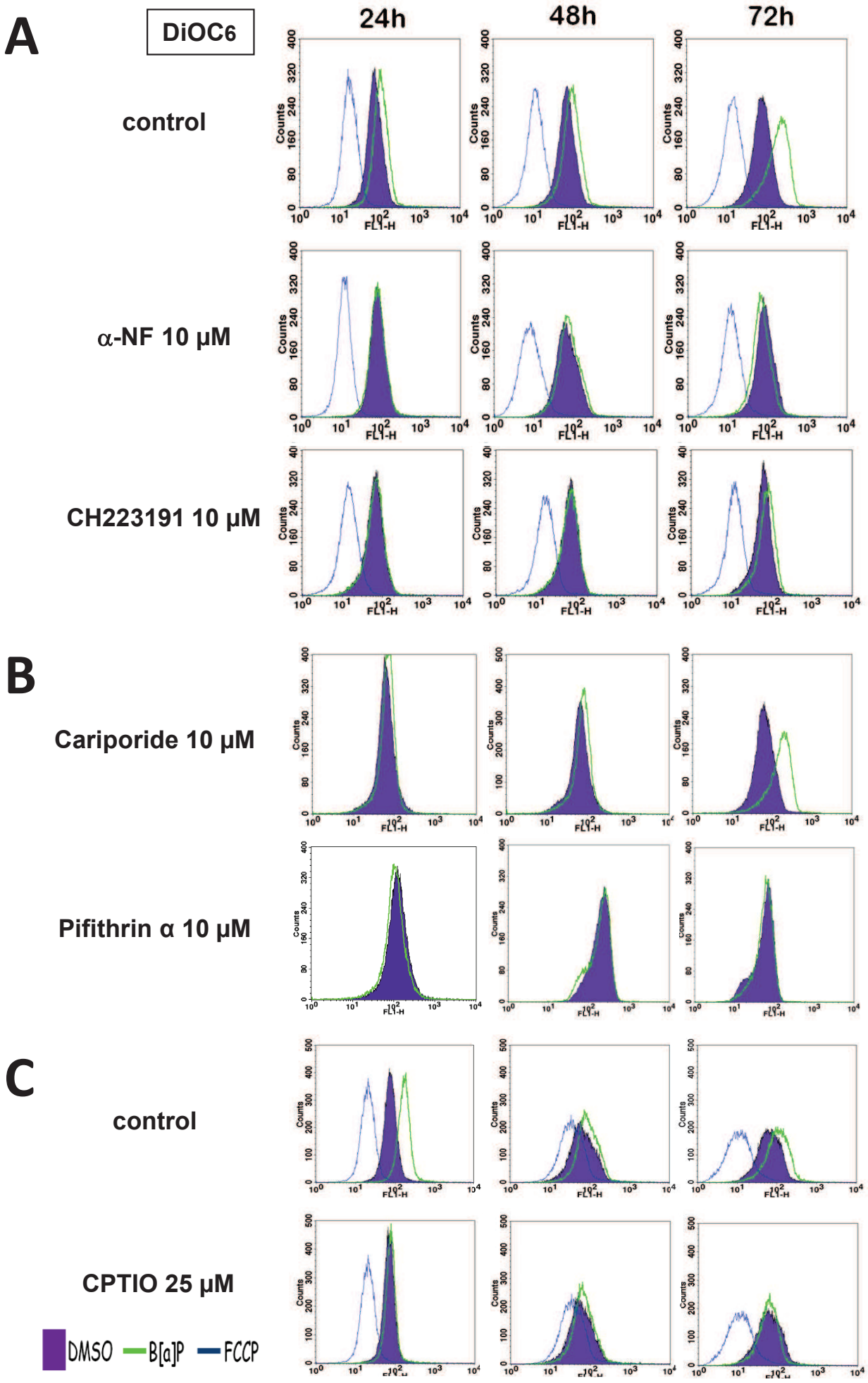

Figure 6

Figure 7

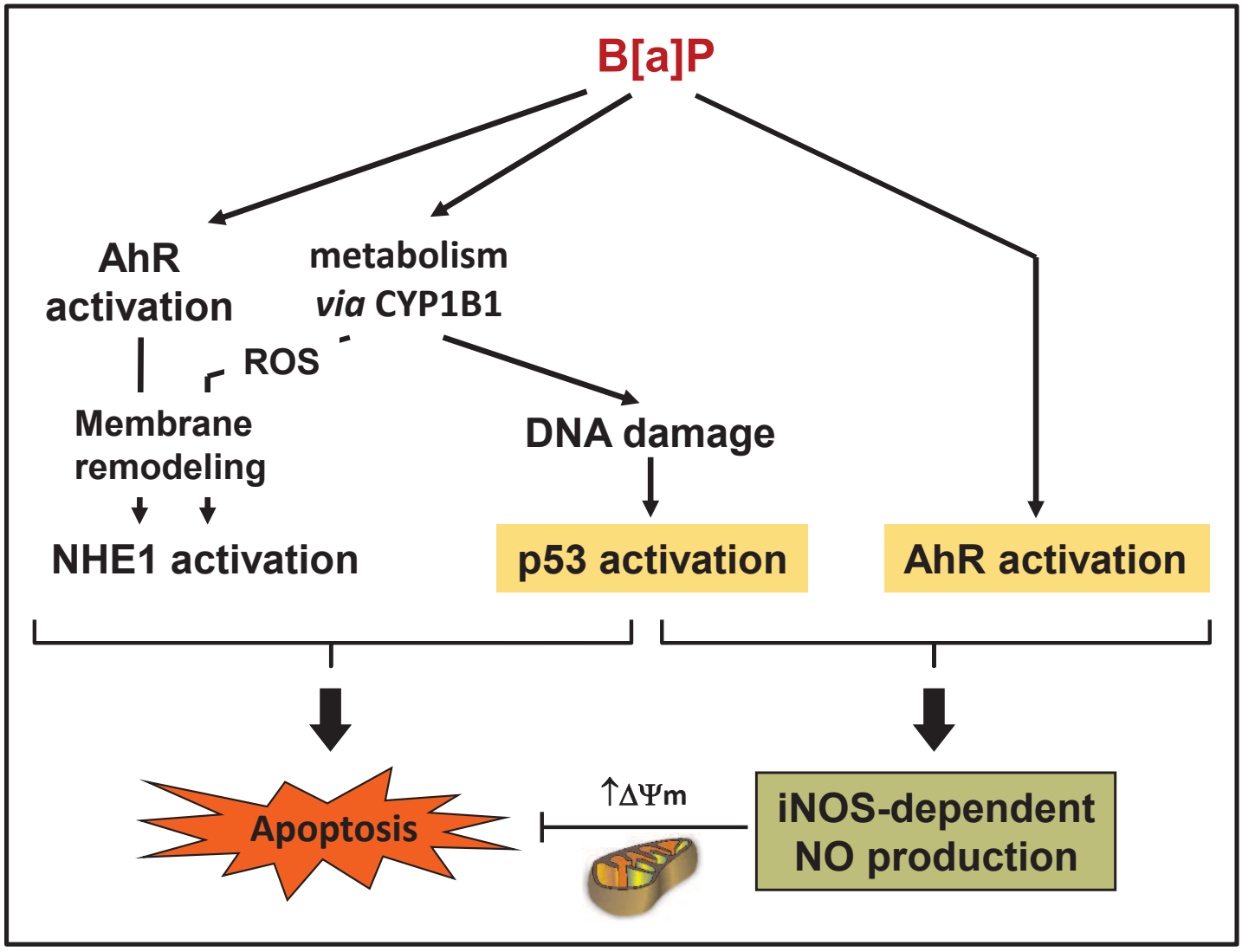

Figure 7

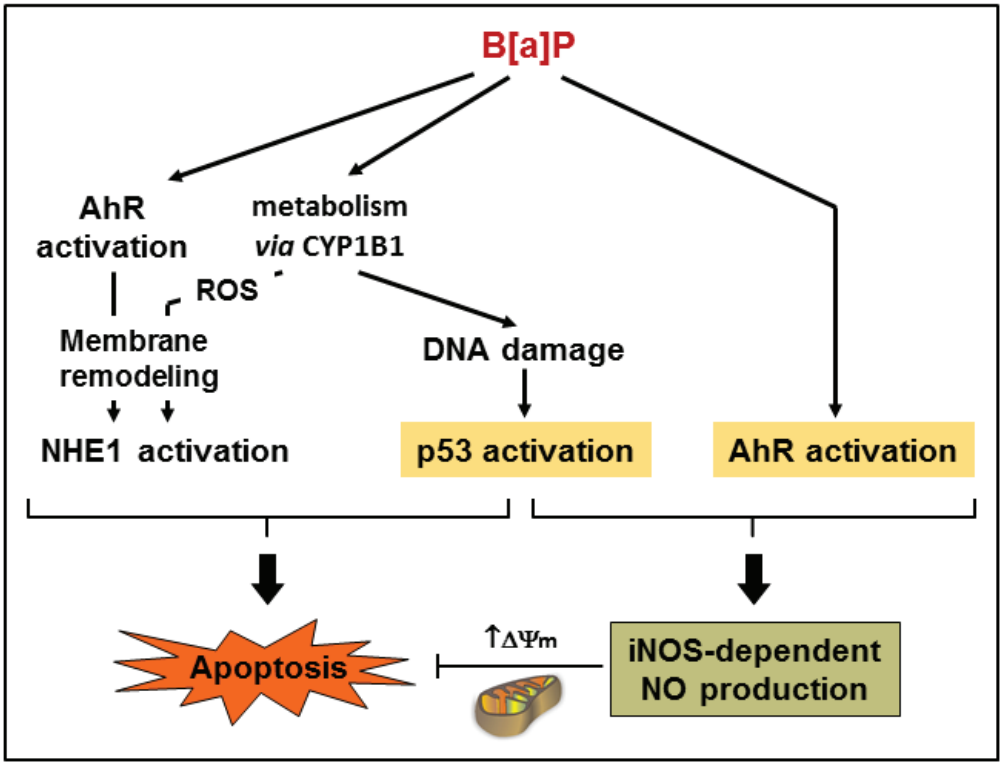

Highlights

-B[*a*]P induced an hyperpolarization of mitochondrial membrane potential.

-B[*a*]P-induced hyperpolarization relies upon an AhR-dependent iNOS activation.

-B[*a*]P-induced NO acts as a survival signal *via* targeting mitochondria.